FIVE-MINUTE OSCILLATION: OBSERVATIONS

Robert J. Rutten, Sterrekundig Instituut, Utrecht University

Literature: Stix section 5.1, listed references, ancient essay (in Dutch)

- *discovery*
  - (Plaskett 1954), Leighton et al. 1960
  - chromospheric 3-min: Noyes 1967
- *confusion*
  - restoring force: pressure, gravity, magnetic field?
  - nature: propagating, standing, evanescent?
  - periodicity: piston, cavity, filter?
  - origin: subsurface, surface, atmosphere?
- *enlightenment*
  - prediction: (Leibacher & Stein), Ulrich 1970
  - spherical sun: Wolff 1972, Ando & Osaki 1975
  - identification: (Ulrich & Rhodes), Deubner 1975
- *deployment*
  - helioseismology: low-l networks, South Pole $\Rightarrow$ GONG, SOHO/MDI, SDO
  - time-distance local helioseismology & far-side mapping
  - asteroseismology

1954MNRAS.114..251P

MOTIONS IN THE SUN AT THE PHOTOSPHERIC LEVEL

V. VELOCITIES OF GRANULES AND OF OTHER LOCALIZED REGIONS

H. H. Plaskett

(Received 1954 May 5)

Summary

Velocities and surface brightness in three Oxford spectra, showing granulation, have been measured. The results are in good agreement with those earlier found by Richardson and Schwarzschild in a Mount Wilson spectrum. In two of the three Oxford spectra a significant correlation coefficient of $r=-0{\cdot}28$ has been found between the surface brightness and the sight-line component of the velocity, showing that the bright granular matter is moving vertically upwards. Assuming that the top of the granulation zone occurs at an optical depth of unity, 0·75 km sec^{-1} is a lower limit to the velocity of ascent of the bright granular matter. The smallness, or in one spectrum the absence, of any correlation between surface brightness and velocity suggests that the granular velocities are being partially or completely masked by some other perturbation of velocity. Removing from the observed velocities that part due to granulation, the perturbing velocities are found to originate in an oscillatory velocity field with an average period of 5″ of arc and an amplitude of the order of 0·5 km sec^{-1}.

Leighton, Noyes & Simon 1962ApJ...135..474L

VELOCITY FIELDS IN THE SOLAR ATMOSPHERE
I. PRELIMINARY REPORT*

ROBERT B. LEIGHTON, ROBERT W. NOYES, AND GEORGE W. SIMON
California Institute of Technology, Pasadena, California
Received October 16, 1961

ABSTRACT

Velocity fields in the solar atmosphere have been detected and measured by an adaptation of a technique previously used for measuring magnetic fields Data obtained during the summers of 1960 and 1961 have been partially analyzed and yield the following principal results:

1. Large "cells" of horizontally moving material are distributed roughly uniformly over the entire solar surface. The motions within each cell suggest a (horizontal) outward flow from a source inside the cell. Typical diameters are 1.6×10^4 km; spacings between centers, 3×10^4 km ($\sim 5 \times 10^3$ cells over the solar surface); r.m s. velocities of outflow, 0.5 km sec^{-1}; lifetimes, 10^4–10^5 sec. There is a similarity in appearance to the Ca^+ network. The appearance and properties of these cells suggest that they are a surface manifestation of a "supergranulation" pattern of convective currents which come from relatively great depths inside the sun.

2. A distinct correlation is observed between local brightness fluctuations and vertical velocities: bright elements tend to move upward, at the levels at which the lines Fe λ 6102 and Ca λ 6103 are formed. In the line Ca λ 6103, the correlation coefficient is ~0.5. This correlation appears to reverse in sign in the height range spanned by the Doppler wings of the Na D_1 line and remains reversed at levels up to that of Ca^+ λ 8542. At the level of Ca λ 6103, an estimate of the mechanical energy transport yields the rather large value 2 W cm^{-2}.

3. The characteristic "cell size" of the vertical velocities appears to increase with height from ~1700 km at the level of Fe λ 6102 to ~3500 km at that of Na λ 5896. The r.m s. vertical velocity of ~0 4 km sec^{-1} appears nearly constant over this height range.

4. The vertical velocities exhibit a striking repetitive time correlation, with a period $T = 296 \pm 3$ sec. This quasi-sinusoidal motion has been followed for three full periods in the line Ca λ 6103, and is also clearly present in Fe λ 6102, Na λ 5896, and other lines. The energy contained in this oscillatory motion is about 160 J cm^{-2}; the "losses" can apparently be compensated for by the energy transport (2).

SUPERGRANULATION

Leighton, Noyes & Simon 1962ApJ...135..474L

1. Large "cells" of horizontally moving material are distributed roughly uniformly over the entire solar surface. The motions within each cell suggest a (horizontal) outward flow from a source inside the cell. Typical diameters are 1.6×10^4 km; spacings between centers, 3×10^4 km ($\sim 5 \times 10^3$ cells over the solar surface); r.m s. velocities of outflow, 0.5 km sec^{-1}; lifetimes, 10^4–10^5 sec. There is a similarity in appearance to the Ca^+ network. The appearance and properties of these cells suggest that they are a surface manifestation of a "supergranulation" pattern of convective currents which come from relatively great depths inside the sun.

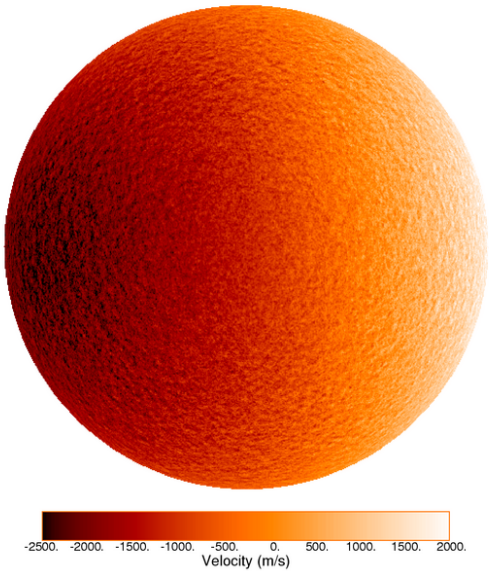

MDI supergranulation movie

SUPERGRANULATION MEASUREMENT

Noyes 1967IAUS...28..293N

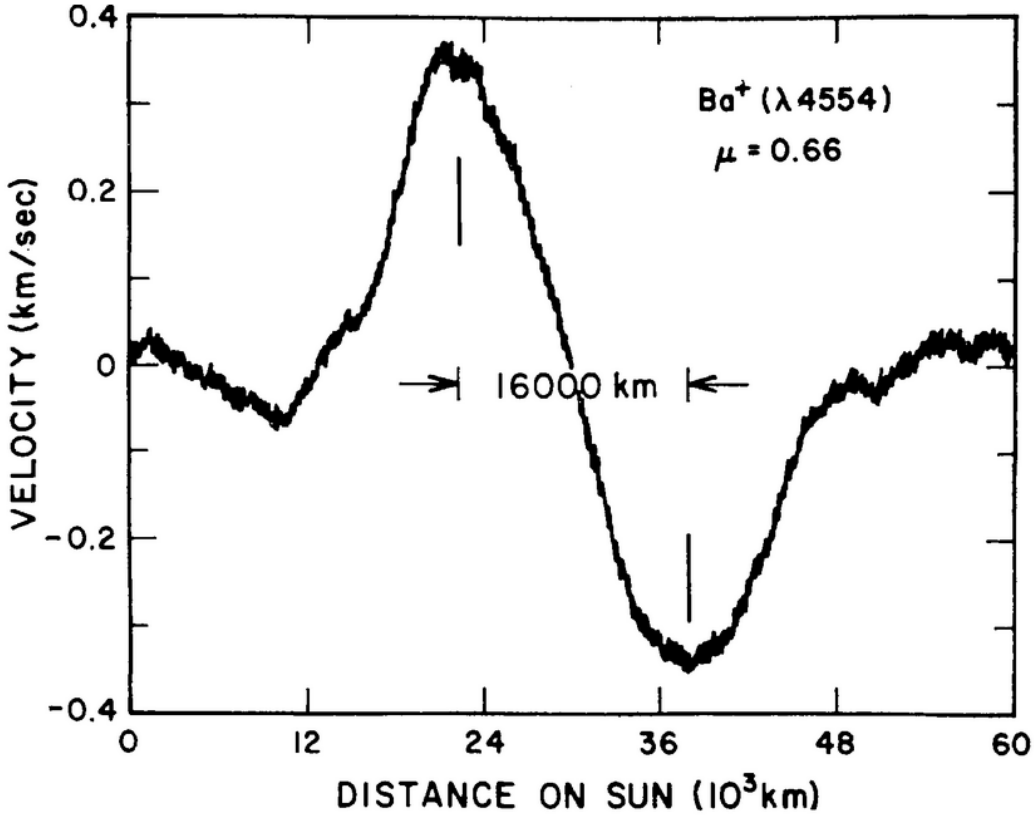

FIG. 8. Microphotometer tracing across an individual supergranulation cell, perpendicular to the solar limb (Simon and Leighton, 1964).

SUPERGRANULATION CARTOON

Noyes 1967IAUS...28..293N

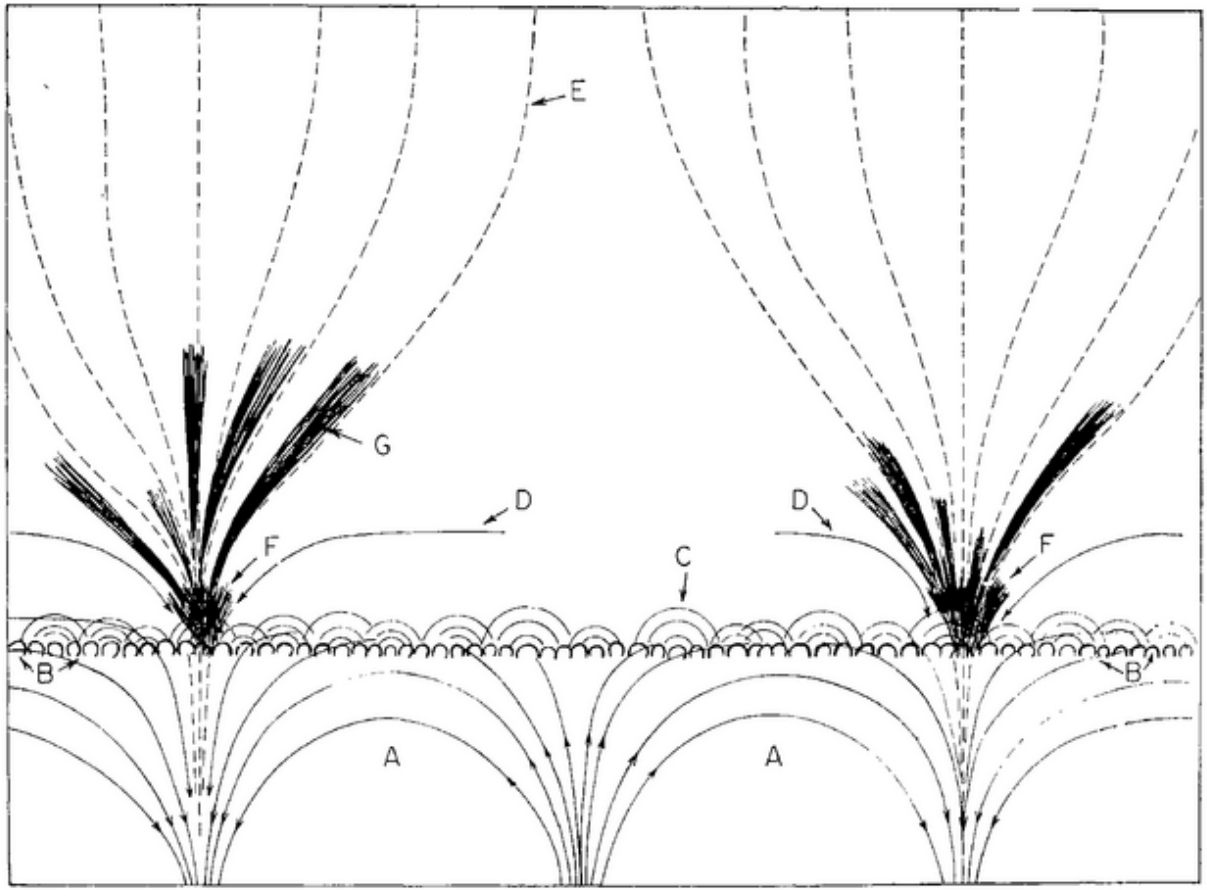

REVERSED GRANULATION

Leighton, Noyes & Simon 1962ApJ...135..474L
Rutten, de Wijn & Sütterlin 2004A&A...416..333R

2. A distinct correlation is observed between local brightness fluctuations and vertical velocities: bright elements tend to move upward, at the levels at which the lines Fe λ 6102 and Ca λ 6103 are formed. In the line Ca λ 6103, the correlation coefficient is ∼0.5. This correlation appears to reverse in sign in the height range spanned by the Doppler wings of the Na D_1 line and remains reversed at levels up to that of Ca^+ λ 8542. At the level of Ca λ 6103, an estimate of the mechanical energy transport yields the rather large value 2 W cm^{-2}.

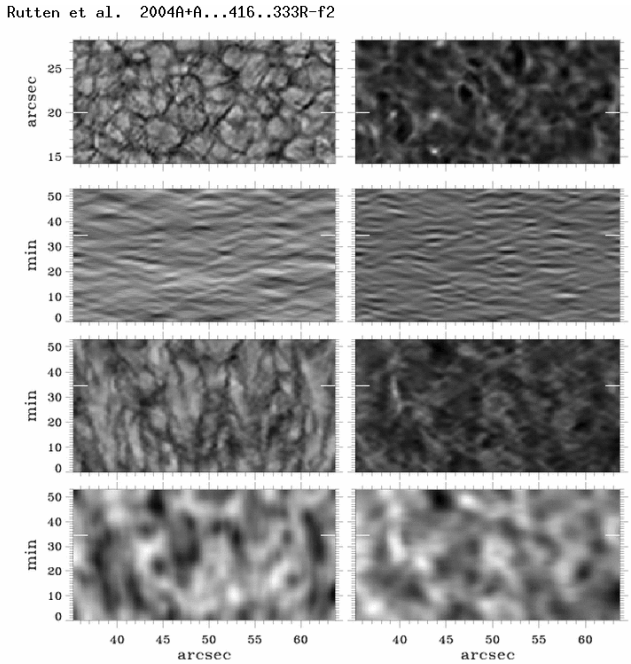

DOT movie 2002-12-08-gb-ca-hi-lo.mpg

REVERSED GRANULATION

Leenaarts & Wedemeyer-Böhm 2005A&A...431..687L

2005A&A...431..687L

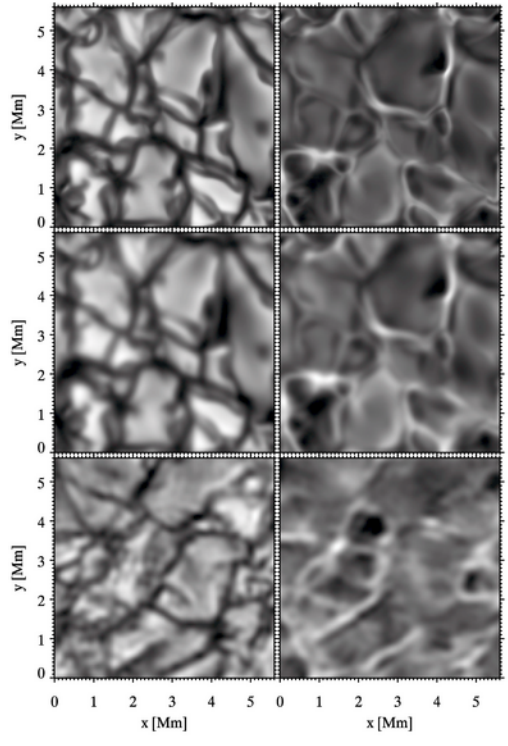

Fig. 1. Simulated and observed images of the blue continuum (left-hand column) and Ca II H wing (right-hand column). The time lag between blue continuum and Ca II H is 120 s for the simulated image pairs and 150 s for the observed pair. *Top row*: simulation data. *Middle row*: simulation data convolved with the best-fit telescope point spread function. *Bottom row*: observations of June 18, 2003. The graininess of the observations is due to camera noise.

FIVE-MINUTE OSCILLATION

Leighton, Noyes & Simon 1962ApJ...135..474L

3. The characteristic "cell size" of the vertical velocities appears to increase with height from ~1700 km at the level of Fe λ 6102 to ~3500 km at that of Na λ 5896. The r.m s. vertical velocity of ~0 4 km sec^{-1} appears nearly constant over this height range.

4. The vertical velocities exhibit a striking repetitive time correlation, with a period $T = 296 \pm 3$ sec. This quasi-sinusoidal motion has been followed for three full periods in the line Ca λ 6103, and is also clearly present in Fe λ 6102, Na λ 5896, and other lines. The energy contained in this oscillatory motion is about 160 J cm^{-2}; the "losses" can apparently be compensated for by the energy transport (2).

5. A similar repetitive time correlation, with nearly the same period, seems to be present in the *brightness fluctuations* observed on ordinary spectroheliograms taken at the center of the Na D_1 line. We believe that we are observing the transformation of potential energy into wave energy through the brightness-velocity correlation in the photosphere, the upward propagation of this energy by waves of rather well-defined frequency, and its dissipation into heat in the lower chromosphere.

MDI Doppler movie

DOT movie 2002-12-08-gb-hi-lo-smooth.mpg

CHROMOSPHERIC DYNAMICS

Leighton, Noyes & Simon 1962ApJ...135..474L

6. Doppler velocities have been observed at various heights in the upper chromosphere by means of the Hα line. At great heights one finds a granular structure with a mean size of about 3600 km, but at lower levels one finds predominantly *downward* motions, which are concentrated in "tunnels" which presumably follow magnetic lines of force and are geometrically related to the Ca^+ network. The Doppler field changes its appearance *very rapidly* at higher levels, typical lifetimes being about 30 *seconds*.

DOT movie 2004-10-15-filament-4p.mpg: quiet area with filament

DOT movie 2005-07-13-AR10789-gb-caw-hac-had.mpg: quiet region with small spot

SST movie 2005-10-04: active region near limb

PHOTOGRAPHIC DOPPLER ANALYSIS

Leighton, Noyes & Simon 1962ApJ...135..474L

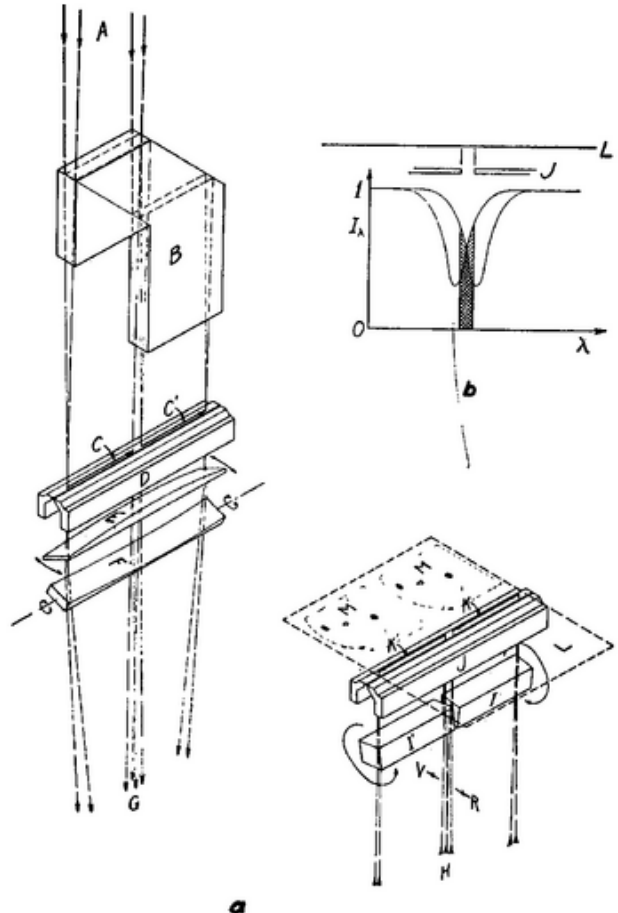

PHOTOGRAPHIC CROSS-CORRELATION

Leighton, Noyes & Simon 1962ApJ...135..474L

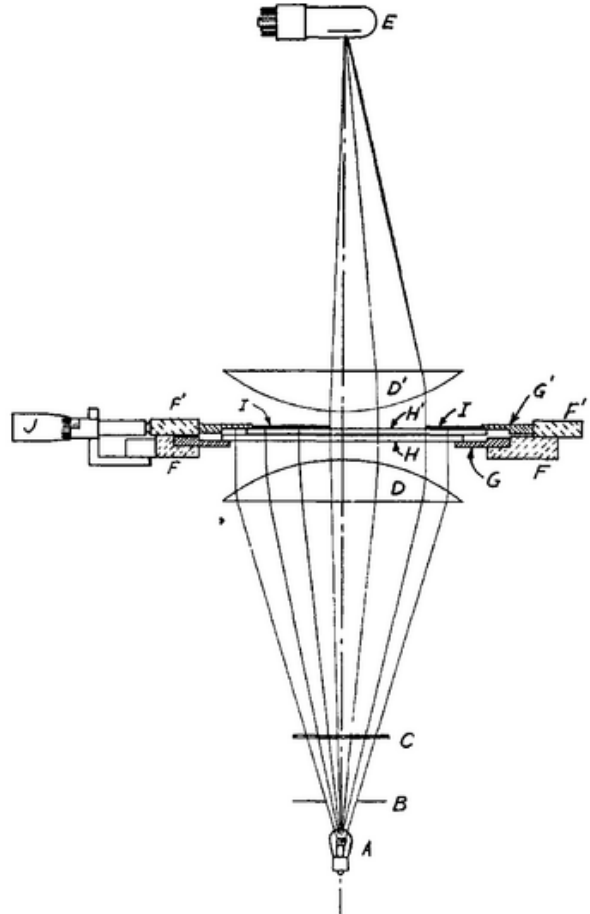

SUPERGRANULATION

Leighton, Noyes & Simon 1962ApJ...135..474L

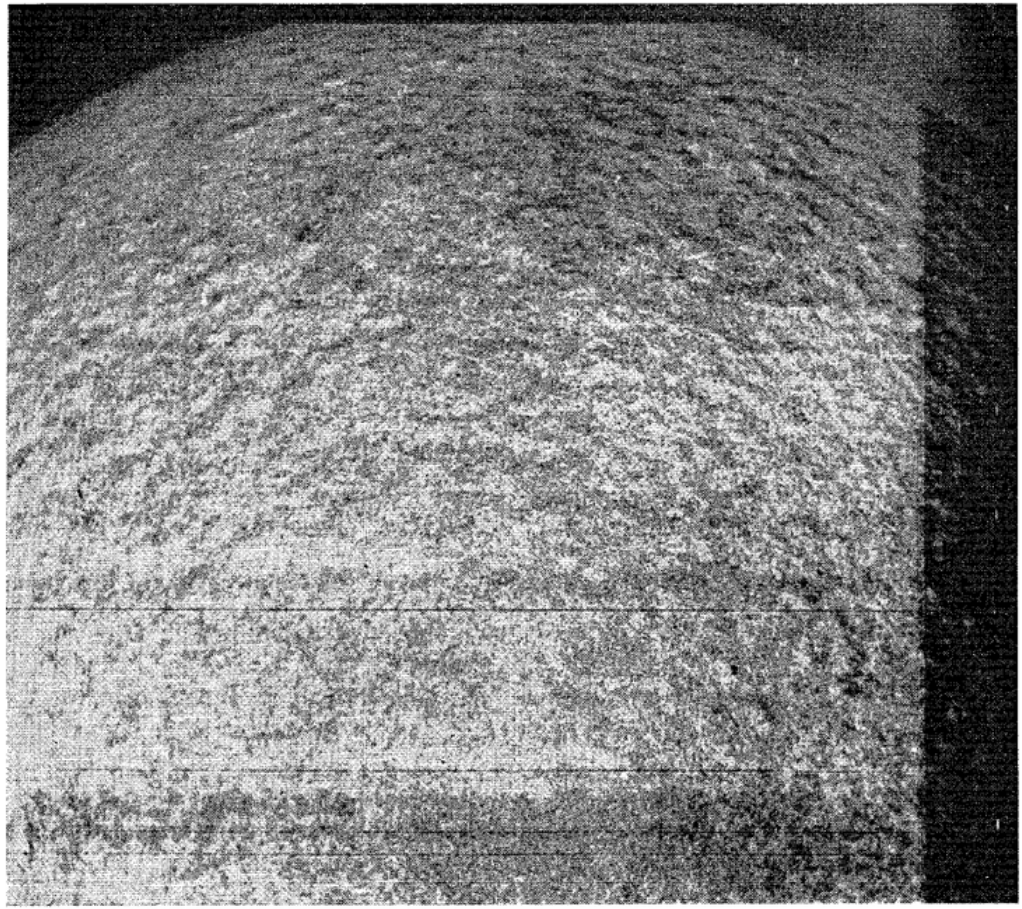

FIVE-MINUTE OSCILLATION

Leighton, Noyes & Simon 1962ApJ...135..474L

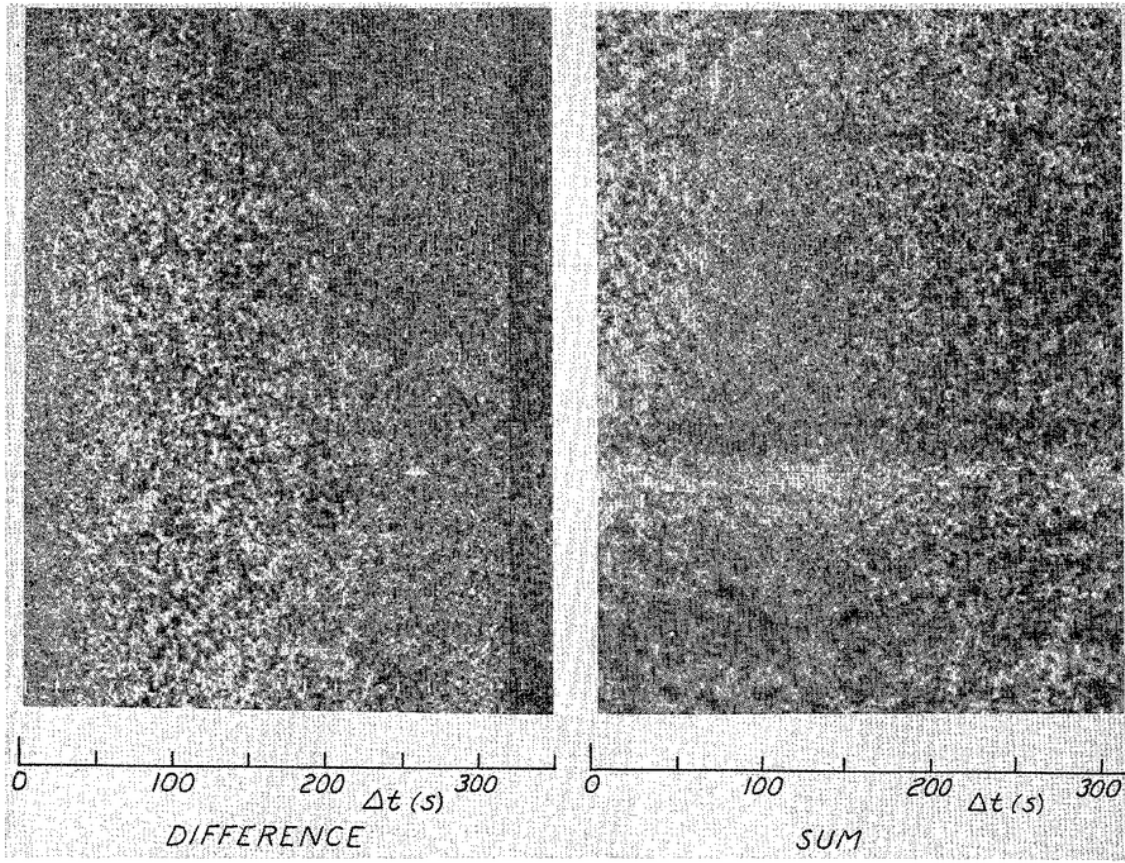

FIG. 17.—Doppler difference (*left*) and sum (*right*) plates, in the line Ba^{+} 4554. July 1, 1961, $13^{h}55^{m}$ U.T.

OSCILLATION POWER WITH HEIGHT

Noyes 1967IAUS...28..293N

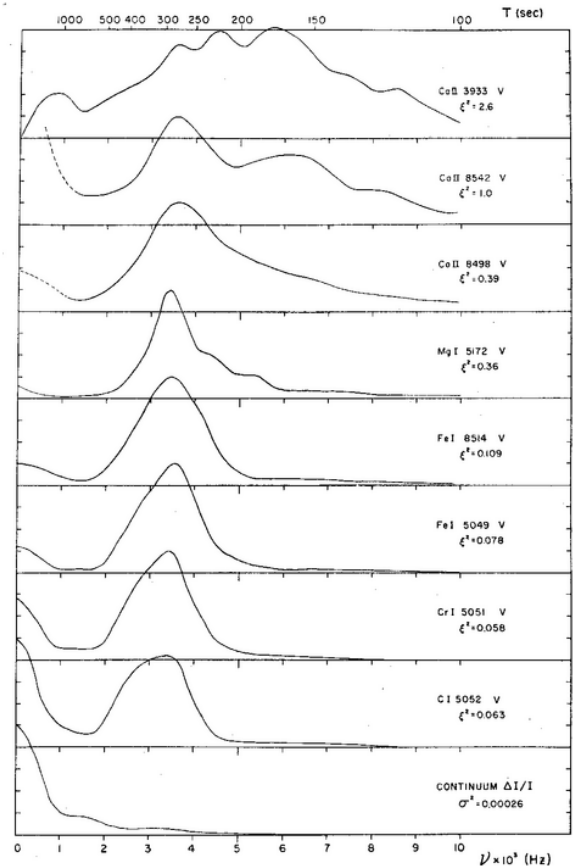

CHROMOSPHERIC THREE-MINUTE OSCILLATION

Cram *1983ApJ...272..355C*

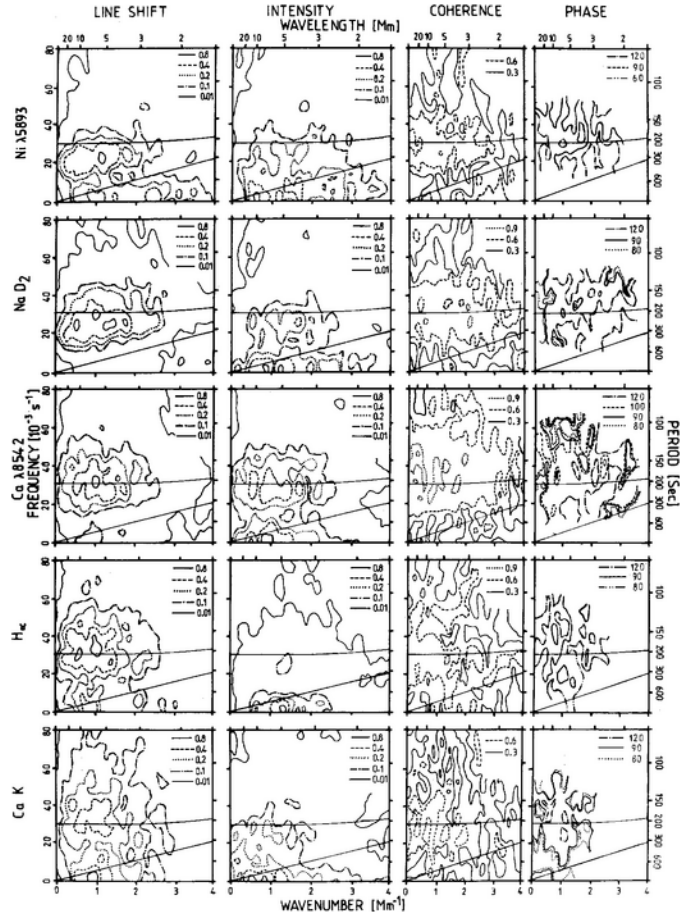

FIVE MINUTE OSCILLATION WAVETRAINS

Stein & Leibacher 1974ARA+A..12..407S

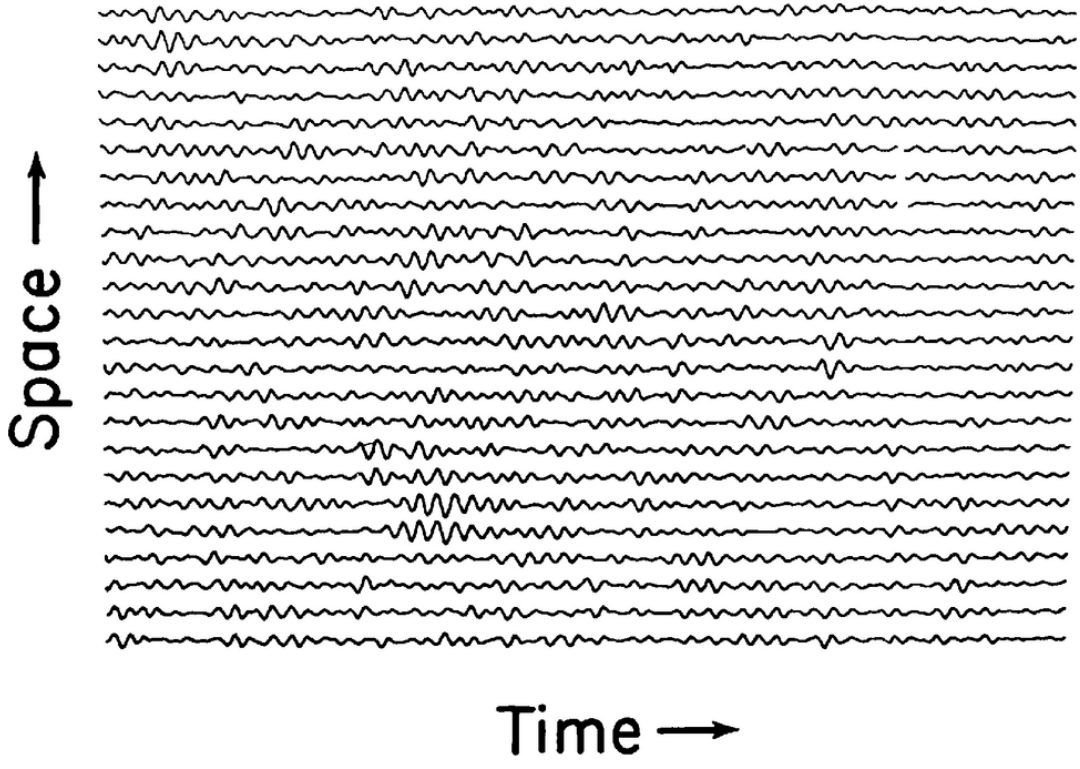

FIVE MINUTE OSCILLATION AS RANDOM PHENOMENON

White & Cha 1973SoPh...31...23W, 1973SoPh...31...55C

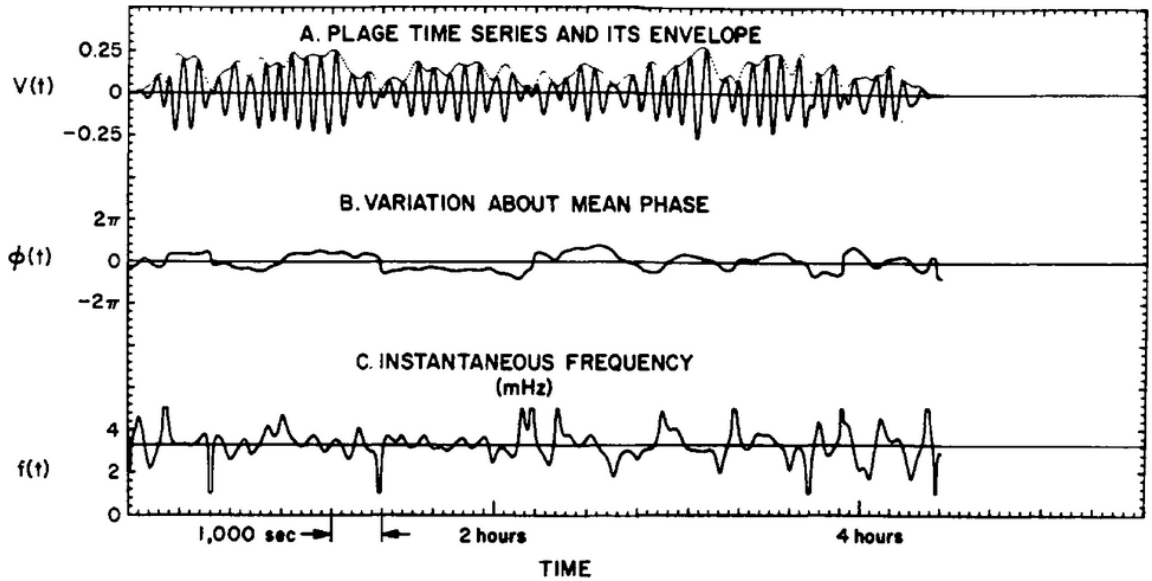

Abstract. Four Mt. Wilson measurements ($T > 4$ h) of the photospheric motion at one point on the Sun are shown to have the characteristics of a narrow-band random process. The motion is shown to have a characteristic correlation time of 23 min and a mean power spectrum that is a smooth, single-peaked function centered at 3.4 mHz. In order to make this classification we use the *analytic signal* to estimate the amplitude, phase, and frequency as functions of time. The power spectrum analysis differs from the common approaches in that it uses the theoretical expression for the mean spectrum for a sequence of random pulses. Because of the random nature of the motion, we doubt the existence of more than one eigenfrequency characteristic of the photosphere as a whole. Likewise, any description of the observed motion in terms of simple deterministic functions will be inadequate for the data used here.

DIAGNOSTIC DIAGRAM

Pierre Mein 1966AnAp...29..153M

Le troisième chapitre comporte une étude statistique bidimensionnelle des séquences d'observation mentionnées plus haut. Les résultats sont traduits dans le diagramme diagnostique (fréquence — nombre d'onde sur le disque solaire). Les spectres de puissance obtenus permettent l'étude de l'évolution du champ de vitesses avec l'altitude, en comparaison avec la théorie des ondes. Des ondes évanescentes sont probablement responsables des oscillations de moyenne fréquence ($T \sim 300$ s); le domaine des ondes acoustiques reste sans doute limité aux périodes inférieures à 240 s pour les altitudes envisagées ; quant à la présence d'ondes de gravité, elle n'est pas incompatible avec les résultats obtenus pour les perturbations de basse fréquence, bien qu'il semble plus vraisemblable d'attribuer à ces perturbations un caractère convectif.

Section three consists of a two-dimensional statistical study of the above-mentioned observational sequences. The results are given in the diagnostic diagram (frequency — wave number on the solar disk). With the power spectra obtained, the evolution of the velocity field with height may be studied and compared with wave theory. Evanescent (stationary) waves are probably responsible for oscillations of moderate frequency ($T \sim 300$ s); the region of acoustic waves is apparently limited to periods less than 240 s for the heights considered; as far as gravity waves are concerned, their presence is not incompatible with results obtained for low frequency perturbations, although it seems more realistic to treat these perturbations as convective in character.

DIAGNOSTIC DIAGRAM

Pierre Mein 1966AnAp...29..153M

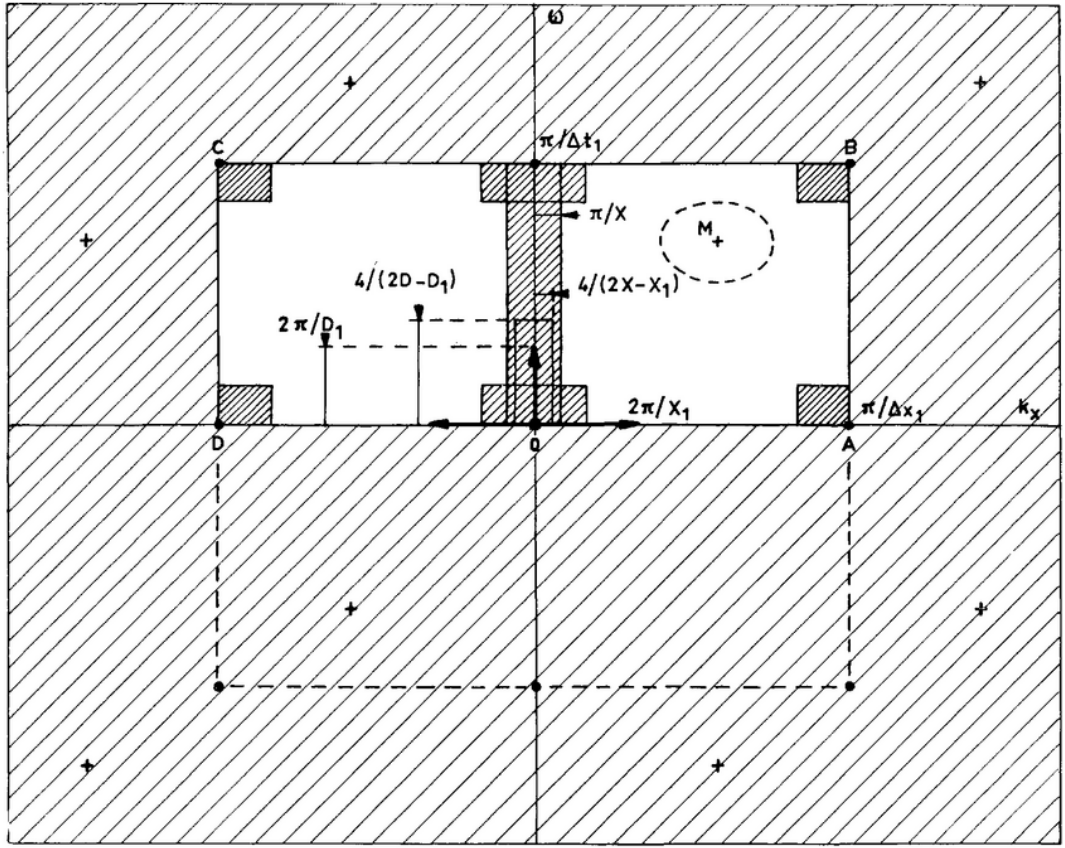

FIG. 6. — Domaines de définition du spectre $F_1(k_x, \omega)$. Le calcul est dépourvu de sens physique ou imprécis dans les zones hachurées ; les flèches représentent sensiblement les « éléments spectraux ».

DIAGNOSTIC DIAGRAM

Pierre Mein 1966AnAp...29..153M

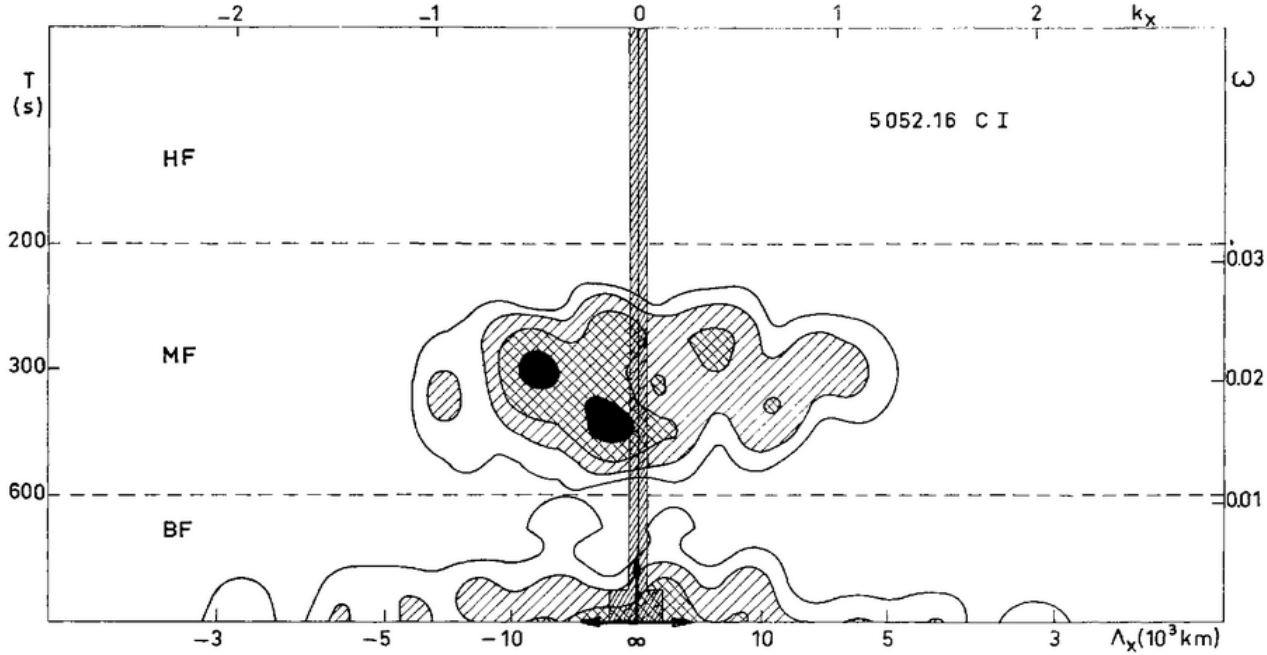

FIG. 7. — Spectre de puissance des vitesses (raie 5052 C I) dans le plan (k_z, ω). Les courbes de niveau correspondent aux produits de la valeur maximale par 0,1 ; 0,2 ; 0,4 ; 0,8. Les flèches représentent les éléments spectraux.

DIAGNOSTIC DIAGRAM

Pierre Mein *1966AnAp...29..153M*

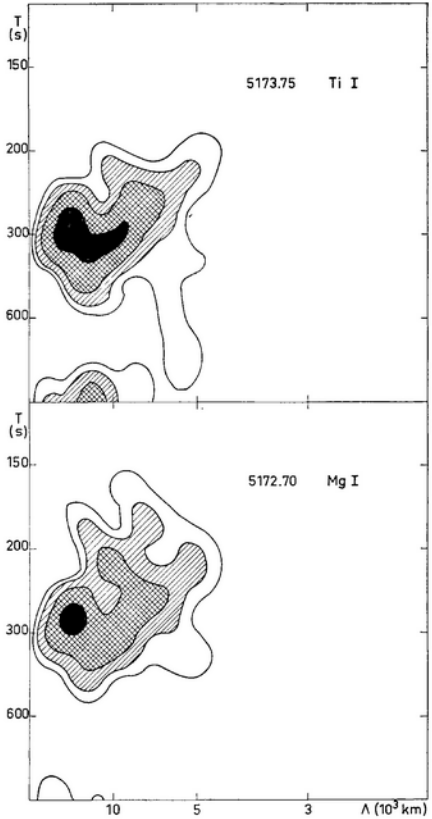

FIG. 9. — Spectres de puissance dans le plan (k, ω) relatifs aux vitesses observées pour les 8 échantillons. Les axes sont gradués en longueurs d'onde horizontales et en périodes. Les courbes de niveau correspondent aux produits des valeurs maximales par 0,1 ; 0,2 ; 0,4 ; 0,8.

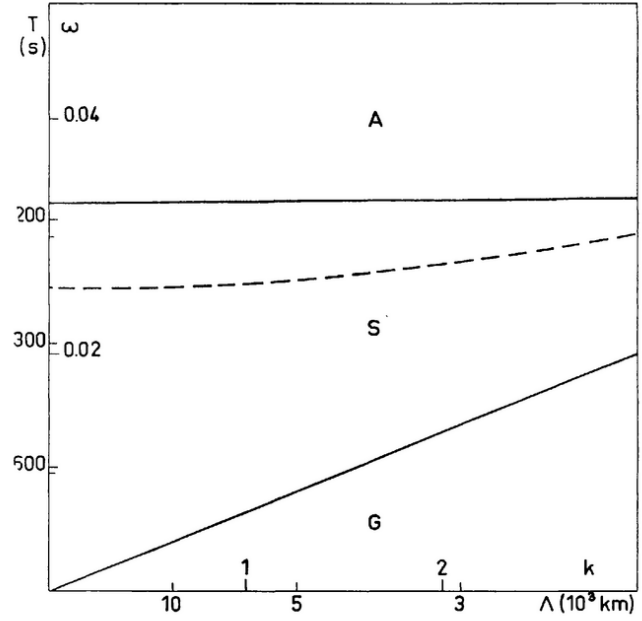

FIG. 11. — Diagramme diagnostique dans le cas solaire pour une température moyenne de 5000 °K. La portion de plan (k, ω) représentée est la même que dans la figure 9.

FIVE MINUTE OSCILLATION K–OMEGA

Frazier 1968ZA.....68..345F
Stein & Leibacher 1974ARA+A..12..407S

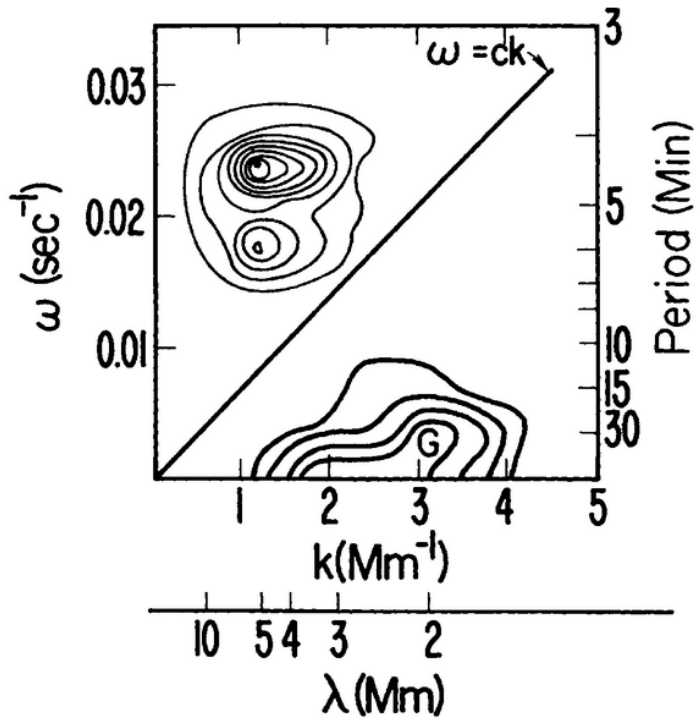

Figure 6 Observed velocity power spectrum in Fe I 6355. The cutoff at small k_x is caused by the size (7 Mm) of the region observed, and the cutoff at large k_x is caused by atmospheric seeing. The extension of low frequency power (G) resembles an internal-gravity modal curve. (Frazier 1968b, reprinted by permission from *Z. Ap.*)

p-MODE CONFUSION

Deubner 1972SoPh...22..263D

The most interesting results are the following:

(1) The 5-min oscillations appear in our power spectra as smooth peaks, although the spectra would easily resolve e.g., a double peak structure like that in Frazier's spectra. The appearance of multiple peaks (in smaller samples) does not depend on high spatial resolution. On the other hand we have new arguments that even a $10'' \times 10''$ area is not large enough a sample of the solar surface to provide statistical stability. We therefore conclude that only observations which cover the duration of several wavetrains at many physically independent positions – an area of $100'' \times 100''$ observed for 2 hr might be appropriate – give us a consistent picture of the average dynamical properties of the solar photosphere. Nevertheless, it will be still interesting to study carefully the properties of isolated wave trains in order to learn more about their propagation and their possible sources. The low photospheric layers, where the oscillations are less ubiquitous, provide a suitable layer for such studies.

(2) Large wavelengths of $30''$ to $60''$ are found to be most prominent among the 5-min oscillations in the $k-\omega$ power spectra. This agress with earlier measurements from which a phase coherence length comparable to supergranular size had been derived. These wavelengths are compatible with a model which assumes an oscillatory field consisting of statistically independent elements with a $10''$ to $20''$ diameter. It is

FIVE MINUTE OSCILLATION: FIRST LIGHT

Ulrich 1970ApJ...162..993U

THE FIVE-MINUTE OSCILLATIONS ON THE SOLAR SURFACE*

ROGER K. ULRICH
University of California, Los Angeles
Received 1970 March 5; revised 1970 June 3

ABSTRACT

The acoustic properties of the subphotospheric layers are examined. It is shown that standing acoustic waves may be trapped in a layer below the photosphere. These standing waves may exist only along discrete lines in the diagnostic diagram of horizontal wavenumber versus frequency. The positions of these lines are derived from a modal analysis of the solar envelope The lines for the fundamental mode and the first-overtone mode pass through the centers of the two peaks observed by Frazier. An examination of the energy balance of the oscillations shows that they are overstable. When they are assigned an amplitude of 0.2 km sec^{-1}, they generate about (5–7) $\times$ 10^6 ergs cm^{-2} sec^{-1}. This power output suggests that the dissipation of the 5-minute oscillations above the temperature minimum is responsible for heating the chromosphere and corona.

I would like to thank Dr. E. N. Frazier for suggesting that the 5-minute oscillations might be dependent on the subphotospheric layers. I am grateful to Professor R. F. Christy for suggesting that my unexpected result that the oscillations are self-exciting might be more than a numerical error. I wish to thank the Kellogg Laboratory at Caltech for their hospitality and support during the initial phases of this work.

FIVE MINUTE OSCILLATION: FIRST LIGHT

Ulrich 1970ApJ...162..993U

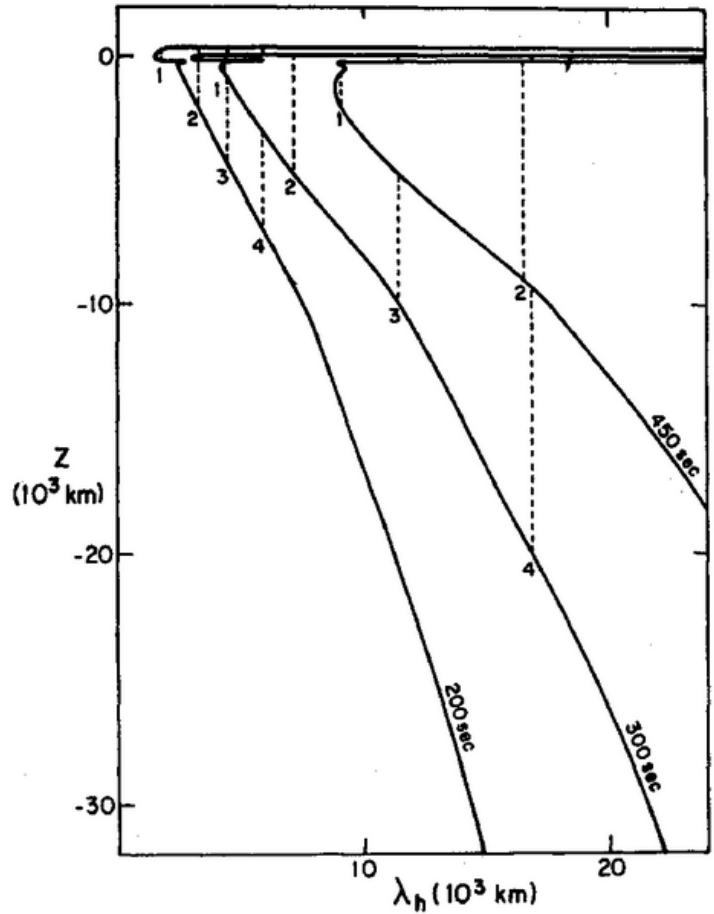

FIVE MINUTE OSCILLATION: FIRST LIGHT

Ulrich 1970ApJ...162..993U

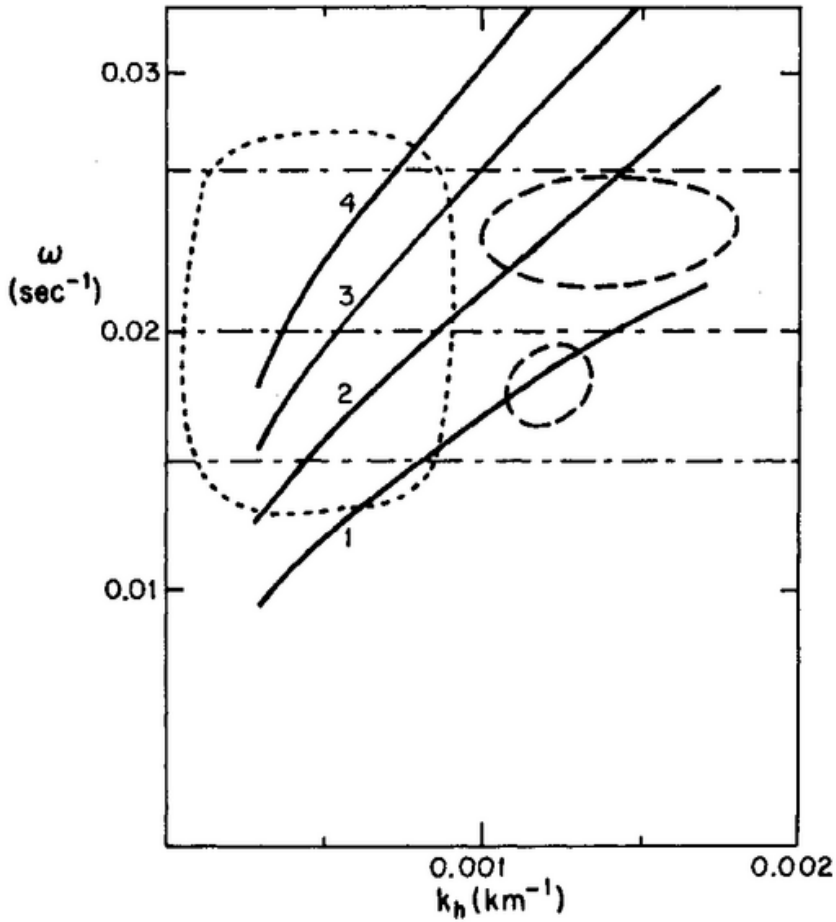

THE SUN IS A SPHERE

Wolff 1972ApJ...177L..87W

THE FIVE-MINUTE OSCILLATIONS AS NONRADIAL PULSATIONS OF THE ENTIRE SUN

CHARLES L. WOLFF
Laboratory for Solar Physics, NASA-Goddard Space Flight Center, Greenbelt, Maryland 20771
Received 1972 June 23; revised 1972 August 14

ABSTRACT

Calculations of the stability coefficient show that the Sun should be pulsating as a unit in nonradial modes of high order. The pulsations are driven by the superadiabatic gradient of the low photosphere and by the same sensitive changes in opacity that are known to be important in variable stars. The existence of solar pulsations can explain many of the large scale features observed in the well known 5-minute oscillations of the solar atmosphere.

An obvious way to test this theory is to search for velocities distributed over the solar surface according to some spherical harmonic. Because of the long wavelengths involved, fairly large scanning elements $\sim 10^2$ square seconds of arc can be used, and this would have the added advantage of diminishing the relative contribution of the solar granulation noise. But the data for the spatial analysis must be carefully restricted to narrow bands of acoustical frequencies; otherwise, one will average over many modes and obtain only the transient and complicated patterns which have been seen many times before. If solar pulsations can be monitored with enough precision, they will ultimately prove valuable probes of the solar interior structure and will place additional experimental limits on stellar convection theory.

THE SUN IS A SPHERE

Wolff 1972ApJ...177L..87W

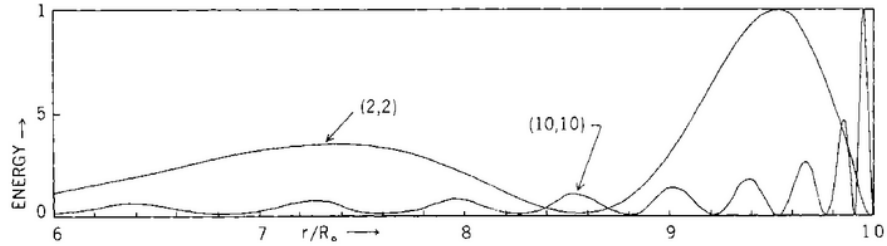

FIG. 1.—Radial distribution of kinetic energy (arbitrary units) in spherical shells of unit thickness for two nonradial *p*-modes of solar oscillation.

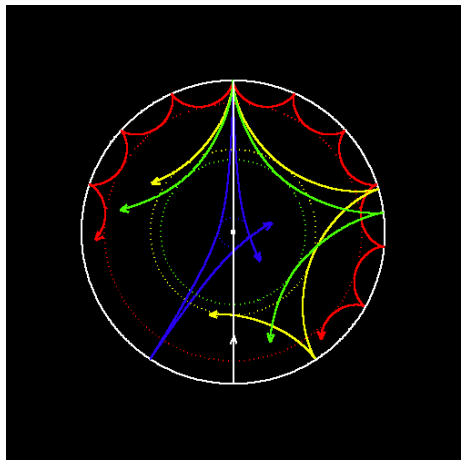

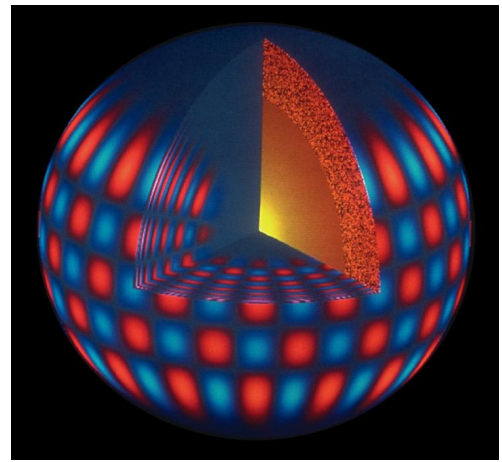

NUMERICAL p-MODE PREDICTION

Ando & Osaki 1975PASJ...27..581A

The stability of acoustic modes trapped in the solar convection zone is studied by solving the equations of linear nonadiabatic nonradial oscillations. The radiative transfer of perturbations is treated by the Eddington approximation which can be applied both for the optically thick and thin cases. The growth or damping rates of oscillations are determined from the imaginary part of eigenfrequency. The results are shown in the diagnostic (k_x, σ)-diagram, where k_x is the horizontal wave number and σ is the angular frequency of oscillations. It is found that many of the acoustic modes are overstable and that the most unstable modes occupy a long mountain-range-like region in the (k_x, σ)-diagram centered with a period of 300 s and with a wide range of horizontal wavelength, which is in good agreement with observations of the five-minute oscillation. It is shown that the driving of oscillations is mainly due to the κ-mechanism of the hydrogen ionization zone, while the radiation loss in the optically thin layers contributes appreciably to the damping.

(a) *Basic Equations and Boundary Conditions*

The basic equations governing nonadiabatic radial pulsations in the radiative atmosphere were formulated by UNNO (1965), in which the radiative transfer was treated in the Eddington approximation. UNNO and SPIEGEL (1966) have demonstrated that the Eddington approximation in the radiative heat equation is very useful in three-dimensional time-dependent problems. We thus utilize this in the present paper. The basic equations governing nonadiabatic nonradial oscillations in the radiative atmosphere are then given as

$$\frac{\partial \rho}{\partial t}+\boldsymbol{\nabla}\cdot(\rho \boldsymbol{v})=0\,, \tag{1}$$

$$\frac{d\boldsymbol{v}}{dt}=-\frac{1}{\rho}\boldsymbol{\nabla}P-\boldsymbol{g}\,, \tag{2}$$

$$c_P\rho\left(\frac{dT}{dt}-\nabla_{\rm ad}\frac{T}{P}\frac{dP}{dt}\right)=-\pi\boldsymbol{\nabla}\cdot\boldsymbol{F}\,, \tag{3}$$

$$\boldsymbol{F}=-\frac{4}{3\kappa\rho}\boldsymbol{\nabla}J\,, \tag{4}$$

and

$$J=\frac{ac}{4\pi}T^4+\frac{c_P}{4\pi\kappa}\left(\frac{dT}{dt}-\nabla_{\rm ad}\frac{T}{P}\frac{dP}{dt}\right), \tag{5}$$

NUMERICAL p-MODE PREDICTION

Ando & Osaki 1975PASJ...27..581A

We assume as usual that the small perturbation of a physical quantity f is written as

$$\left.\begin{matrix} f'(r,\theta,\varphi,t) \\ \delta f(r,\theta,\varphi,t) \end{matrix}\right\} = \left.\begin{matrix} f'(r) \\ \delta f(r) \end{matrix}\right\} Y_l^m(\theta,\varphi)e^{i\sigma t}\,, \tag{6}$$

where (r,θ,φ) is the spherical polar coordinates, the Eulerian and the Lagrangian perturbations are denoted by prime ($'$) and δ, and $Y_l^m(\theta,\varphi)$ is the spherical harmonics. We introduce a nondimensional frequency ω and five nondimensional variables x, p, θ, j, and λ defined by

$$\left.\begin{aligned} &\omega^2=(R^3/GM)\sigma^2\,, \\ &x=\delta r/r\,, \quad p=P'/\rho g r\,, \quad \theta=\delta T/T\,, \\ &j=\delta J/J\,, \quad \lambda=\delta L_r/L_s\,, \end{aligned}\right\} \tag{7}$$

where $L_r=4\pi^2r^2F$ is the luminosity at radius r and L_s is the luminosity at the surface. By linearizing equations (1)-(5), we then obtain four first-order linear differential equations and one auxiliary equation:

NUMERICAL p-MODE PREDICTION

Ando & Osaki 1975PASJ...27..581A

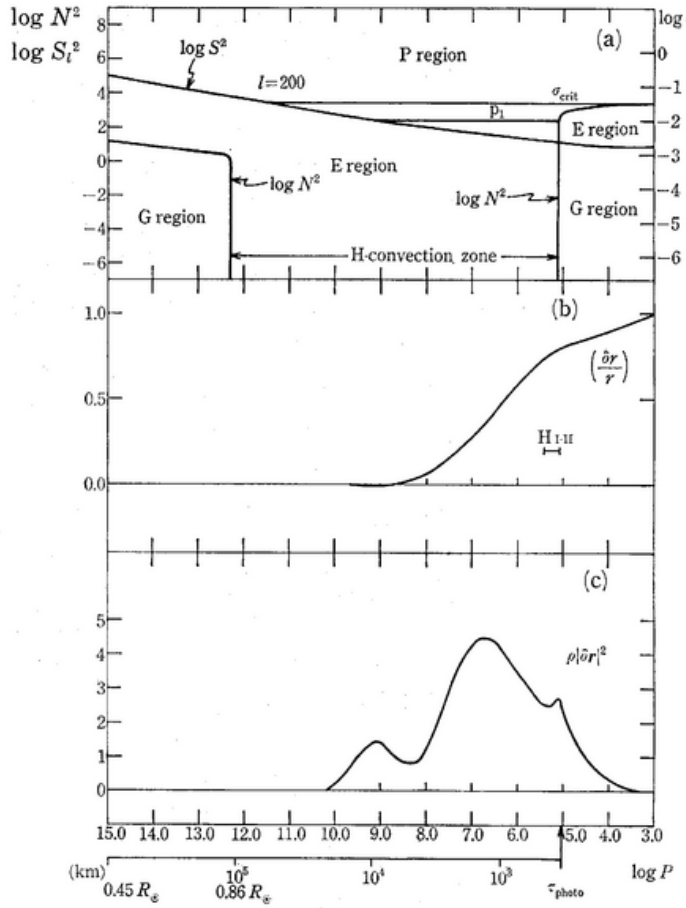

NUMERICAL p-MODE PREDICTION

Ando & Osaki *1975PASJ...27..581A*

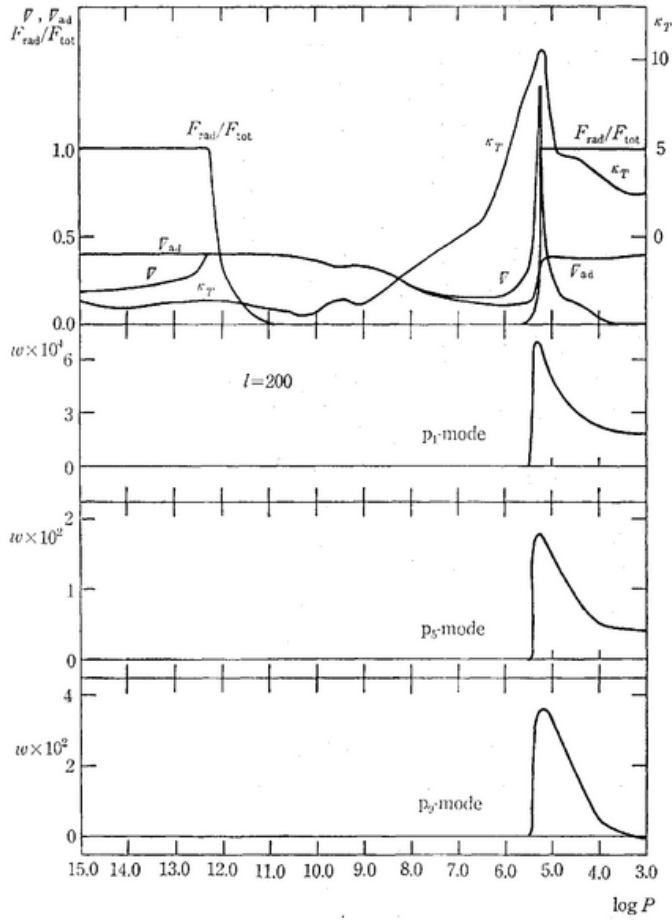

NUMERICAL p-MODE PREDICTION

Ando & Osaki 1975PASJ...27..581A

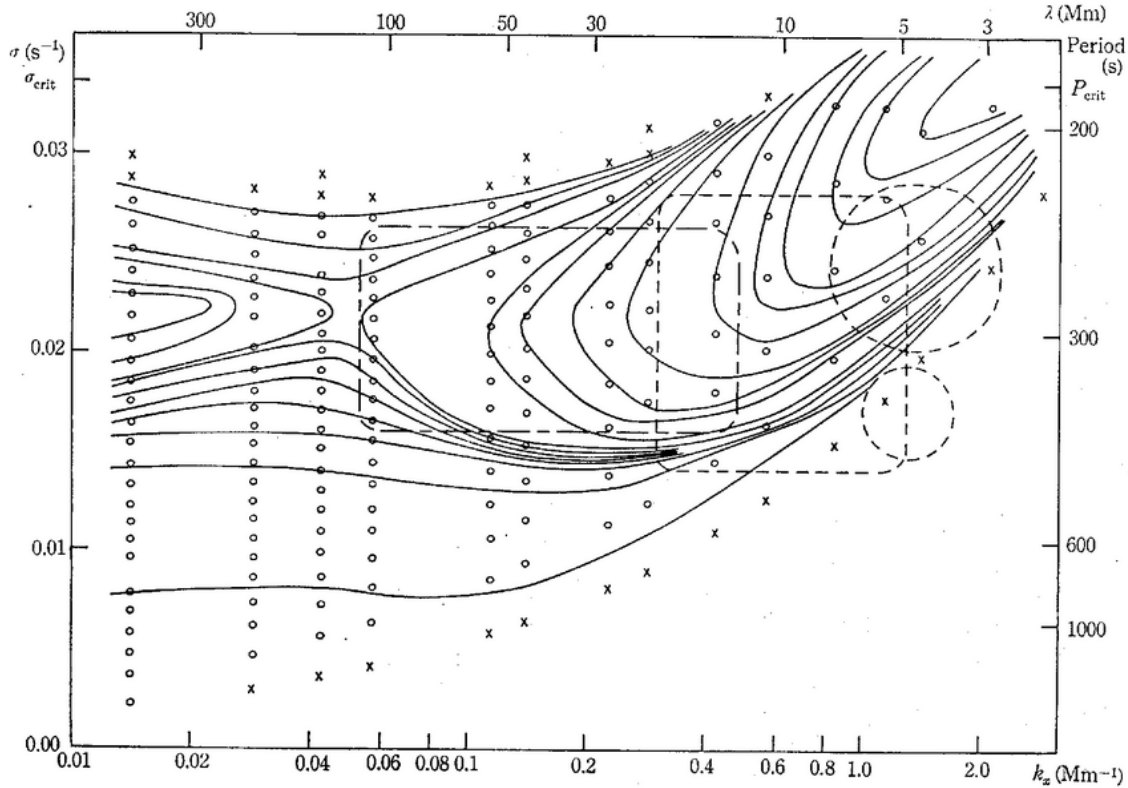

Fig. 7. The diagnostic (k_x, σ)-diagram showing unstable (○) and stable (×) modes. The solid curves show the contour map of equal growth rates η. The regions of observed power of oscillations are also indicated.

p-MODE IDENTIFICATION

Deubner 1975A+A....44..371D

Observations of Low Wavenumber Nonradial Eigenmodes of the Sun*

Franz-Ludwig Deubner
Fraunhofer-Institut, Freiburg i. Br., Fed. Rep. Germany

Received April 10, 1975

Summary. New photoelectric observations of the photospheric velocity field with high resolution in horizontal wavenumber and frequency have been carried out in the CI 5380 line. Three or four discrete stable modes of the five-minute oscillations are resolved in the k, ω diagram, which agree in many respects with the predicted fundamental modes of subphotospheric standing acoustic waves.
Some interesting aspects of the confirmation of a "global" excitation mechanism of the five-minute oscillations are pointed out. Several apparently discordant details of previous observations are rediscussed, and it is shown that they can be reconciled with the present results.

Key words: solar atmosphere — photospheric oscillations — nonradial eigenmodes

p-MODE IDENTIFICATION

Deubner 1975A+A....44..371D

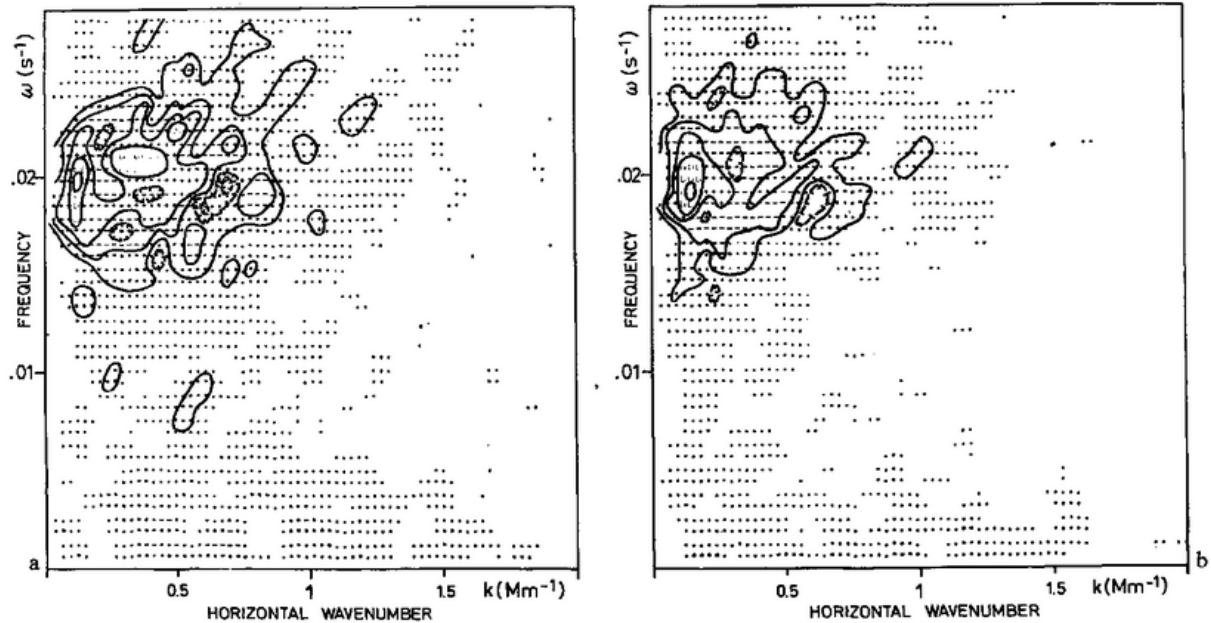

Fig. 1. (a) Diagnostic diagram of the photospheric velocity field computed from Doppler shifts of the CI 5380 line. Six different printer symbols bordered by solid contour lines indicate quadratically increasing levels of kinetic power per unit wavenumber, the lowest level printed (not outlined) being 2.8% of the maximum. Valleys are bordered by broken lines. (b) Same as 1a, obtained with different oriantation of the scan line

p-MODE IDENTIFICATION

Deubner 1975A+A....44..371D

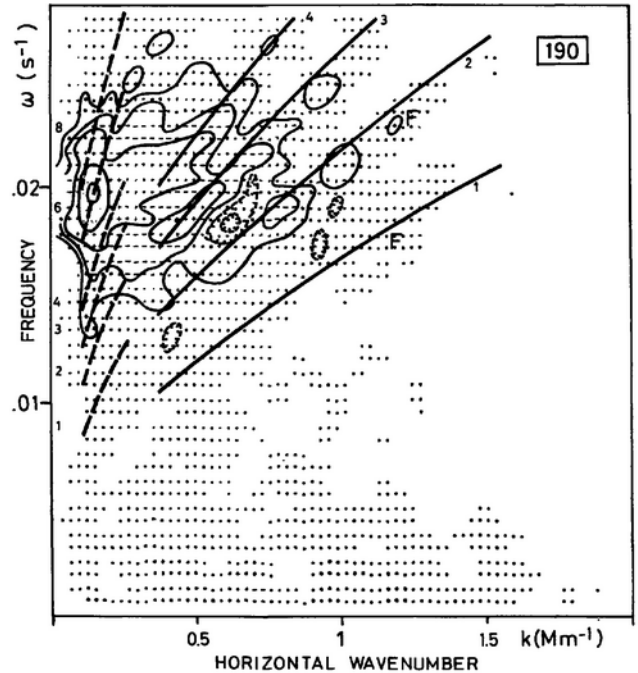

Fig. 2. Diagnostic diagram of the photospheric velocity field obtained by combining the statistically independent power spectra of Fig. 1a and 1b. The spectral resolution element with the number of "degrees of freedom" is given in the upper right corner. Predicted normal modes of trapped acoustic waves are drawn and their radial eigenvalues are given according to Ulrich (solid lines) and Wolff (dashed lines). The two power maxima observed by Frazier (1968) are indicated by a capital *F*

p-MODE IDENTIFICATION

Deubner 1975A+A....44..371D

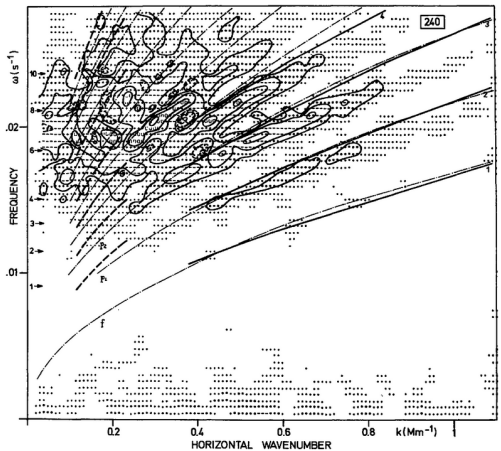

Note: Another set of four-hour recordings of the solar eigenmodes was obtained recently (June 1975) with a larger scan line extending across half the solar diameter. The average k, w diagram resulting from three such recordings is plotted in Fig. 3. Due to the high spectral resolution achieved, more than five modes may be traced down to wavenumbers as low as $0\,\mathrm{s\,Mm^{-1}}$, and can be compared with the theoretical predictions.

We also included in this graph the new results of Ando and Osaki (1975, to be published) who solved the equations of linear *nonadiabatic* nonradial oscillations of the solar envelope. We note that with increasing modal index their solutions (as well as Ulrich's) tend to deviate progressively from the observed positions of the individual

Since the five-minute oscillations very likely contribute significantly to the heating of the upper chromosphere and corona (for a review of literature see Stein and Leibacher, 1974), it seems desirable that the production of this energy flux which has to be supplied continuously and over the whole surface of the sun, does not depend on localized events of a shallow surface layer. The observations provide sufficient evidence that this basic process of the solar envelope is indeed deeply and firmly rooted in the solar body.

p-MODE ROTATION

Deubner, Ulrich & Rhodes 1979A+A....72..177D

Summary. We present new photoelectric observations of the solar p-modes with improved resolution in wave number and frequency. An analysis of the width of the strongest peaks in the k, ω diagram suggests that the p-modes pervade the solar convection zone as a globally coherent phenomenon, Q being probably much larger than 100.

The nodal pattern of the p-modes can be regarded as being "frozen in" at well-defined levels within the convection zone, and therefore, as a tracer of large scale horizontal motions. Differences in the depth dependence of different eigenmodes permit the measurement of the solar rotation rate as a function of depth. The rotation rate is found to be non-uniform, layers at about 15,000 km below the photosphere rotating faster than the surface at about the rotation rate of sunspots.

Summary

The identification of the 5-min oscillations as a global phenomenon which is highly phase coherent in space and time, has given us a tool to observe directly systematic large scale motions in the solar interior. Extension of the present work to solar latitudes other than the equator will eventually provide a quantitative three-dimensional picture of the large scale circulation pattern of the solar interior.

tance of 192″ on the Sun. Three boxes of 32 diodes were placed on either side of the $g=0$, Fe I 5576.099 line.

A bandwidth of 2×76 mÅ in the wings of the line is viewed by each pair of diodes, a band of 76 mÅ at the center of the average position of the line is blocked by a mask. The equivalent width of the spectrograph slit was 2″.

The solar surface was scanned diametrically parallel to the equator from *W* to *E* once every 100 s. The starting position for the scan was continuously shifted westwards at a rate corresponding to the equatorial surface Doppler velocity of rotation. Each scan consists of 544 steps at 1″.825 (=20 guider steps) intervals. The integration time at each position is 133 ms. Including the time for stepping the guider head ($\sim$1000 steps s^{-1}) the total time for a complete scan is about 82 s (without flyback). Every third scan a Ca II K_2 slitjaw filtergram was taken at the center of the flyback motion for reasons explained below. Each of the three observations consists of the tape records of 256 such scans, covering a total of 7.11 h.

Thus, our data reduction procedure comprises basically the following steps:

1. Update the "gaintable" (sensitivity of the 192 individual diodes) every 136 guider steps, as explained in Sect. 2, and correct the raw signals accordingly.
2. For each guider step, and position along the slit, calculate the ratio of the "right wing" to the "left wing" signal.
3. Convert this ratio into a relative velocity by means of the fitted calibration curve (see Sect. 2).
4. For each guider step, calculate the average relative velocity from all 96 pairs of diodes ("long slit").
5. Remove spectrograph drift by subtracting the position of the reference iodine line (Sect. 2) determined from a 9-point fitted parabola, after conversion into a velocity shift.

p-MODE ROTATION

Deubner, Ulrich & Rhodes 1979A+A....72..177D

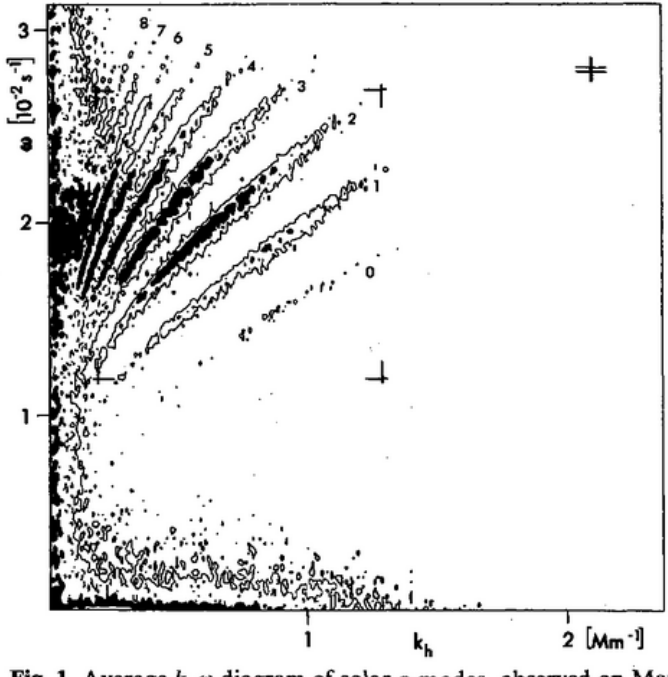

Fig. 1. Average k, ω diagram of solar p-modes, observed on May 6 and 7, 1977. The contours correspond to quadratically increasing relative power levels, the lowest one at 2.8% of maximum power. Power values are multiplied by a factor of $\sqrt{k}$ for conveniant display. The section of the diagram marked by corners was used for the differential rotation analysis. Crossed double bars in the upper right indicate the spectral resolution element $\Delta\omega\Delta k$

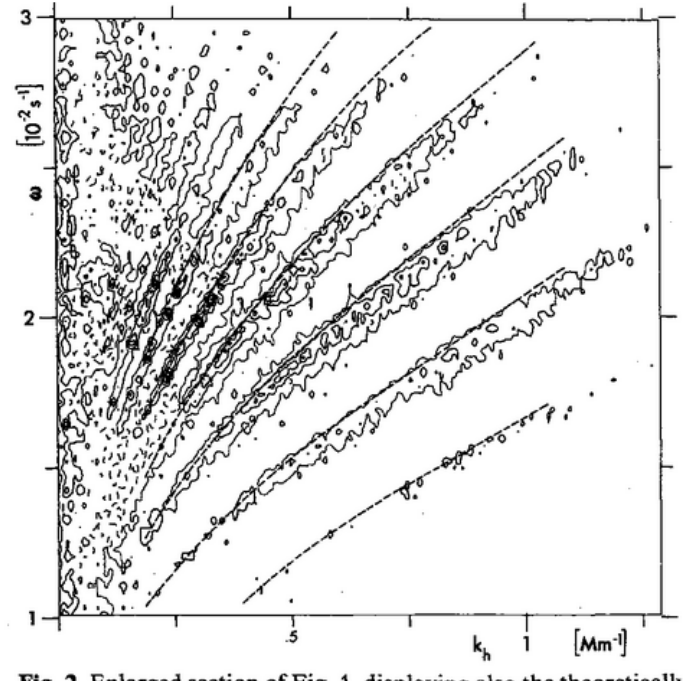

Fig. 2. Enlarged section of Fig. 1, displaying also the theoretically predicted p-modes for a solar envelope model with $l/H = 2$

by the inverse Fourier transform the data were restored into a temporal sequence. (We realize that this procedure is exact only when there is no simultaneous spatial shift $\Delta X(t)$ of the wave

p-MODE ROTATION

Deubner, Ulrich & Rhodes 1979A+A....72..177D

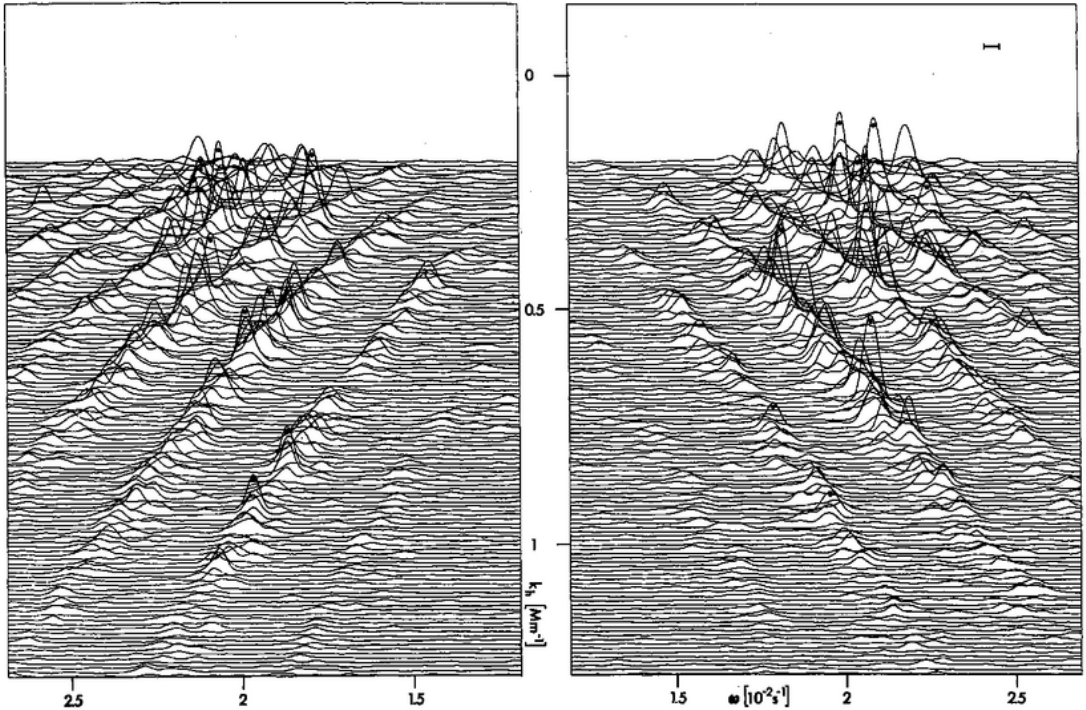

Fig. 3. Section of the k, ω diagram after interpolation of the raw spectral data (see Sect. 3.11), plotted separately for "eastbound" and "westbound" wavetrains, on a linear power scale. 20 peaks, used to determine the width of the p-mode ridges are marked with dots

p-MODE ROTATION

Deubner, Ulrich & Rhodes 1979A+A....72..177D

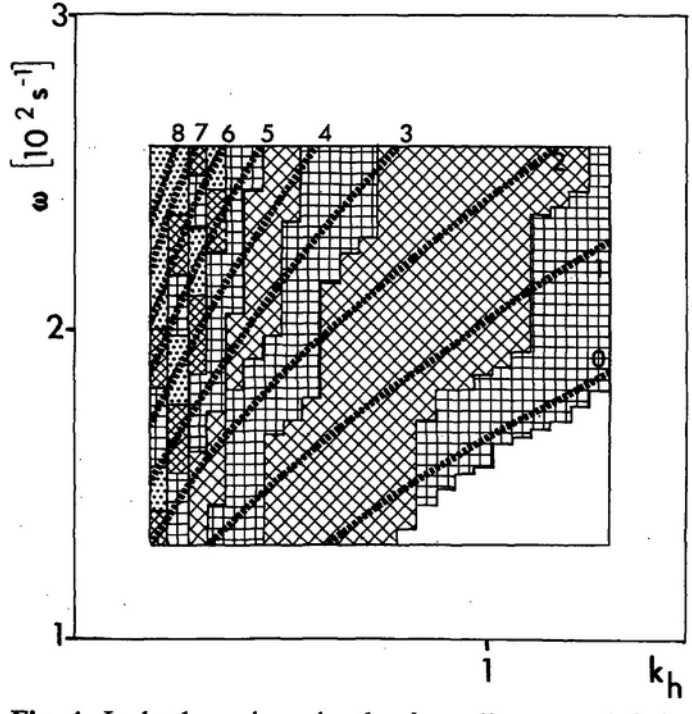

Fig. 4. Isobath regions in the k,ω diagram, defining levels of constant effective depth for the determination of differential rotation. Beginning at the right edge of the diagram 10 different levels are distinguished by different shadings, corresponding to depth ranges from 0–2 Mm, 2–4 Mm, etc. to 18–20 Mm in the upper left corner

p-MODE ROTATION

Deubner, Ulrich & Rhodes 1979A+A....72..177D

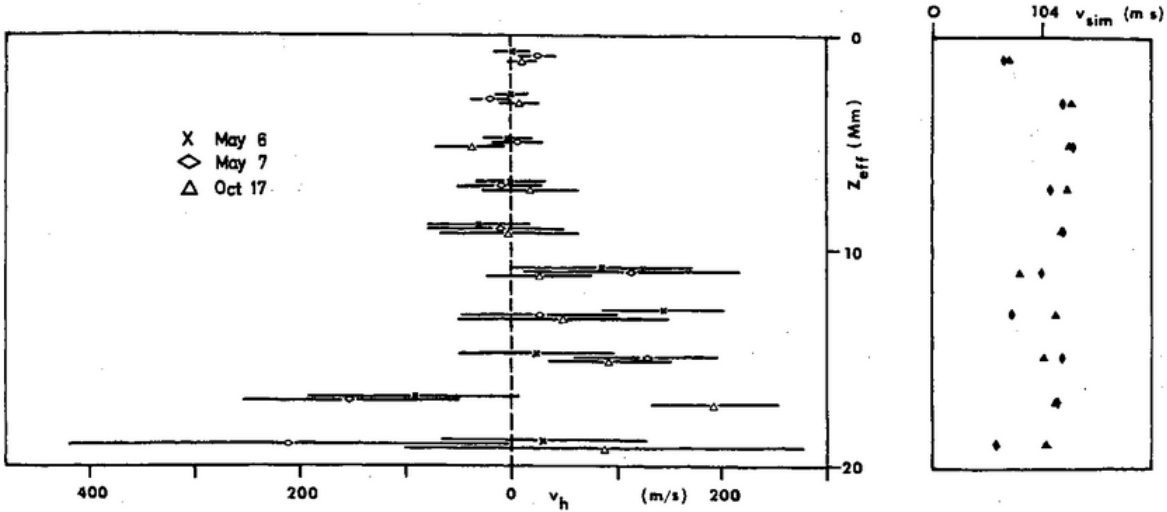

Fig. 5. Observed differential rotation rates as a function of depth below the photosphere. The average rotation rate in the upper four levels (0–8 Mm) is normalized and put equal to zero for each set of observations. Probing the significance of the numerical results, a uniform drift velocity of $+104\ \mathrm{ms}^{-1}$ was introduced numerically into the data sets of May 6 and 7. The results obtained with these faked data are plotted in the small box

SOHO HELIOSEISMOLOGY

http://sohowww.nascom.nasa.gov/gallery/MDI

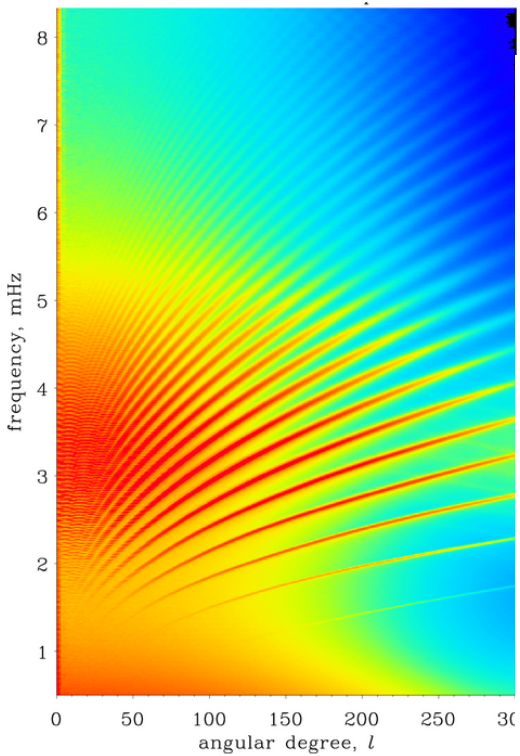

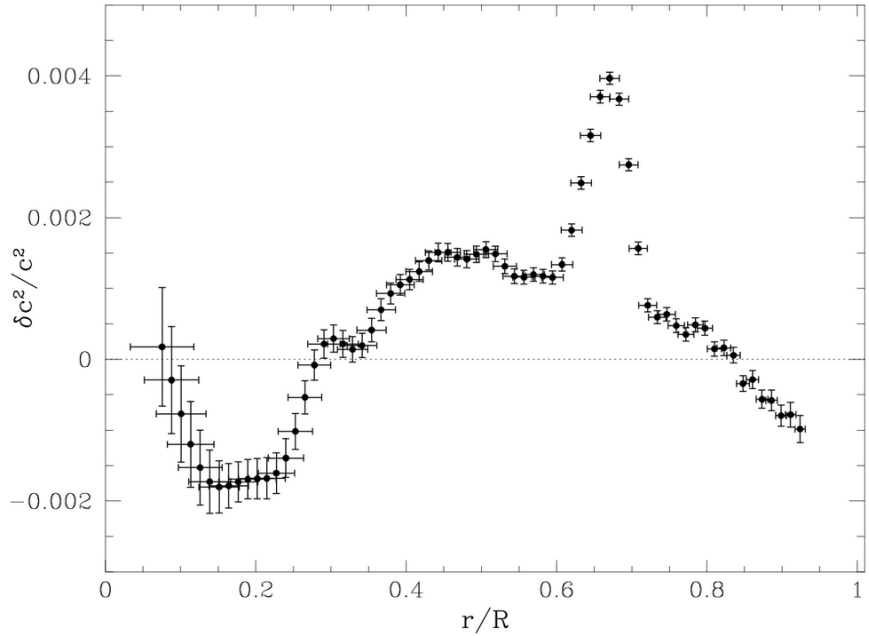

SOHO HELIOSEISMOLOGY

http://sohowww.nascom.nasa.gov/gallery/MDI

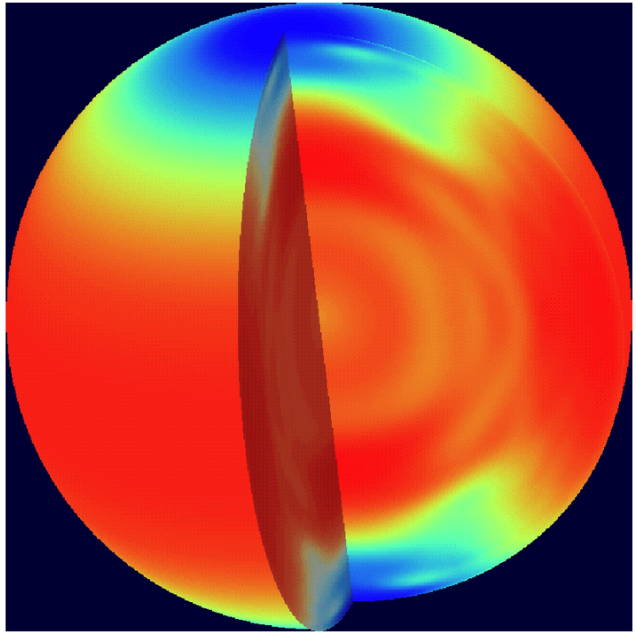

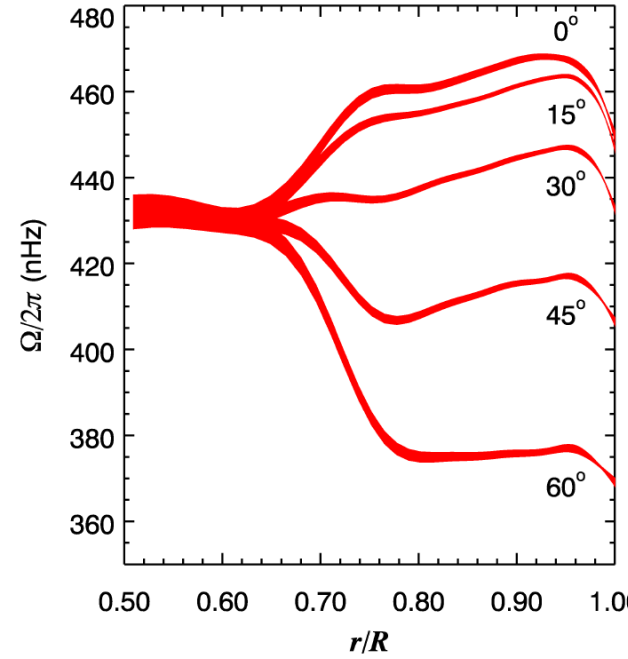

SOHO LOCAL HELIOSEISMOLOGY

http://sohowww.nascom.nasa.gov/gallery/MDI

tachocline movie

local helioseismology

underneath a sunspot

sunspot tomography

AR9393 nearside + backside

PDF SET/DIR FILE TABLE

present talk

talkstart	sol-5minute-plaskett	sol-5minute-leighton1	sol-5minute-leighton2
sol-5minute-noyes-supergran	sol-5minute-noyes-cartoons	sol-5minute-leighton3	sol-5minute-leenaarts-revgran1
sol-5minute-leighton4	sol-5minute-leighton5	sol-5minute-leighton6	sol-5minute-leighton7
sol-5minute-leighton8	sol-5minute-leighton9	sol-5minute-noyes-power	sol-5minute-cram
sol-5minute-wavetrains	sol-5minute-white+cha	sol-5minute-mein1	sol-5minute-mein2
sol-5minute-mein3	sol-5minute-mein4	sol-5minute-frazier	sol-5minute-deubner-no
sol-5minute-ulrich1	sol-5minute-ulrich2	sol-5minute-ulrich3	sol-5minute-wolff1
sol-5minute-wolff2	sol-5minute-ando1	sol-5minute-ando2	sol-5minute-ando3
sol-5minute-ando4	sol-5minute-ando5	sol-5minute-ando6	sol-5minute-deubner1
sol-5minute-deubner2	sol-5minute-deubner3	sol-5minute-deubner4	sol-5minute-deubner-rot1
sol-5minute-deubner-rot2	sol-5minute-deubner-rot3	sol-5minute-deubner-rot4	sol-5minute-deubner-rot5
sol-5minute-deubner-rot6	sol-5minute-soho1	sol-5minute-soho2	sol-5minute-soho3

setfiletable